Feasibility of Nano Electrical Resistive Tomography for Subsurface Atomic Force Microscopy

1st Benjamin J. Stanwell
Precision Mechatronics Lab
University of Newcastle
Newcastle, Australia
benjamin.stanwell@uon.edu.au

2nd Yuen Kuan Yong
Precision Mechatronics Lab
University of Newcastle
Newcastle, Australia
yuenkuan.yong@newcastle.edu.au

3rd Andrew J. Fleming
Precision Mechatronics Lab
University of Newcastle
Newcastle, Australia
andrew.fleming@newcastle.edu.au

2025 IEEE International Conference on Mechatronics (ICM) | 979-8-3315-3389-2/25/$31.00 ©2025 IEEE | DOI: 10.1109/ICM62621.2025.10934851

***Abstract*—This article investigates the feasibility of using a dual-cantilever atomic force microscope for imaging the electrical properties of a sample below the surface. Principles from macro-scale electrical resistive tomography are adapted to utilize measurements from a dual-probe atomic force microscope. A deep-learning method is employed to perform the inversion process and construct the tomography. Simulation results demonstrate that electrical resistive tomography is possible at the nanometre scale but improvements to the inversion algorithms are needed before moving to experimental applications.**

***Index Terms*—Electrical Resistive Tomography, Atomic Force Microscopy, Subsurface**

I. Introduction

Atomic force microscopy (AFM) is a powerful and versatile tool for imaging and surface characterization at the nanoscale [1]. While conventional AFM excels in capturing fine details of surface topography in applications such as materials science [2], biology [3], and nanotechnology [4], understanding subsurface structures is essential for investigating buried defects, layered material interactions, and biological architectures.

Electrical AFM methods generates contrast based on various intrinsic material properties, such as electrical or mechanical characteristics, which can offer insights into both chemical composition and physical structure at the nanoscale [5].

A notable example of an electrical AFM technique is Kelvin probe force microscopy (KPFM) [6], which measures local work function variations by detecting changes in capacitance between the probe and sample. While KPFM is particularly useful for studying surface potential, it is significantly influenced by surface conditions, such as contaminants or surface roughness, which can obscure or distort material contrast [7].

Other emerging methods, like scanning near-field ultrasound holography (SNFUH) [8], extend the reach of SPM by capturing mechanical interactions between the probe tip and sample, potentially offering insights into material elasticity and other mechanical properties. However, these techniques face challenges in interpreting contrast, as the exact contrast mechanisms and their sensitivity to different material properties are not yet fully understood [5], [9].

A. Contributions

This article investigates the feasibility of electrical resistance tomography (ERT) at the nanometre scale for subsurface imaging using a dual-probe AFM. The proposed method, referred to as nano-ERT, aims to reconstruct a three-dimensional image of the sample, where the contrast is resistivity. To improve the numerical efficiency of the inversion process, a deep learning technique is proposed. Deep learning offers a powerful means to solve inverse problems [10] by learning mappings directly from data, making it well-suited to reconstruct the underlying resistive tomography. Occam's inversion [11] for ERT can be computationally expensive and time-intensive, especially for complex materials and geometries. In contrast, once trained, a deep learning model can rapidly generate reconstructions, enabling near-real-time imaging capabilities for AFM-based subsurface imaging. This efficiency is beneficial for applications requiring high-throughput analysis or where rapid feedback is crucial, such as defect inspection in semiconductor manufacturing or in-situ analysis of biological samples. Subsequently Occam's inversion, refines this initial estimate by learning to correct errors or enhance resolution in areas where deep learning may falter.

II. Nano ERT

This section introduces the concept of nanoscale electrical tomography and describes the forward model and associated limitations.

A. Measurement Setup

As illustrated in Figure 1, two AFM probes are positioned above the surface of the sample, with their exact locations described by Cartesian position vectors $\mathbf{r}_+$, $\mathbf{r}_-$. These probes are electrically connected to a test fixture designed to measure resistance. See Figure 1. By adjusting the positions of $\mathbf{r}_+$ and $\mathbf{r}_-$ along the sample surface, spatially-resolved electrical characteristics can be measured. This allows for the mapping of resistivity as a function of position across the sample.

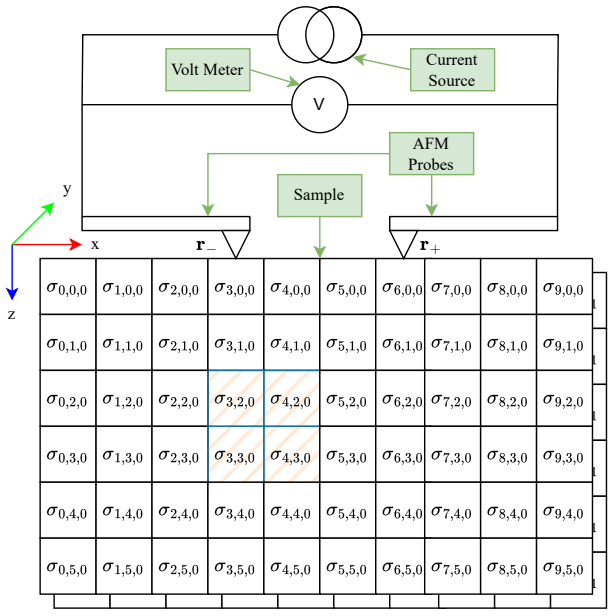

Fig. 1: Dual-probe AFM setup with probes electrically connected to a precision current source and voltmeter, enabling the mapping of subsurface resistivity as discrete voxels within a Cartesian coordinate system

B. Forward Problem Formulation

ERT measures voltages over a surface from a series of input currents. The voltage (V) and currents (I) are related by the Poisson equation [12]

$$-\nabla \cdot (\nabla V)\frac{1}{I} = (\delta(\mathbf{r}-\mathbf{r}_+) - \delta(\mathbf{r}-\mathbf{r}_-)) \cdot \rho(\mathbf{r}) \tag{1}$$

where $\mathbf{r}_+$ and $\mathbf{r}_-$ refer to the probe locations and δ refers to the point source of the probes. Measurements can be viewed as a pseudo-resistance $(\frac{V}{I})$, which is a function of the resistivity $\rho(\mathbf{r})$. The resistance function may also be interpreted as a conductivity function

$$\rho(\mathbf{r}) = \frac{1}{\sigma(\mathbf{r})} \tag{2}$$

C. Inverse Formulation

To formulate an inverse problem, the voltage measurements are mapped to a data vector $\mathbf{d}$ and the resistivity of a material is mapped to a model vector $\mathbf{m}$. The data vector $\mathbf{d}$ is related to the model $\mathbf{m}$ through the forward operator F, that is

$$\mathbf{d} = F(\mathbf{m}) \tag{3}$$

If provided with the data vector $\mathbf{d}$ and forward operator F, the solution for $\mathbf{m}$ is not unique [10]. There is no direct inverse operator and the task instead is to optimise a model $(\mathbf{m}_{est})$ to match observed data $(\mathbf{d}_{obs})$. The misfit function to minimize is

$$\phi_d(\mathbf{m}) = \frac{1}{2}||\mathbf{W}_d(F(\mathbf{m}) - \mathbf{d}_{obs})||^2 \tag{4}$$

where $\mathbf{W}_d$ is a weighting matrix that adjusts the importance of different measurements, based on the uncertainty of the measurements. As the problem is not unique, the inversion may be improved by a regularisation term, that is

$$\phi_m(\mathbf{m}) = \frac{1}{2}||\mathbf{W}_m(\mathbf{m} - \mathbf{m_{ref}})||^2 \tag{5}$$

where $\mathbf{W}_m$ is a weighting matrix similar to $\mathbf{W}_d$, but instead based on uncertainty in the model. Regularization terms can quantify prior information known about the model.

With the inclusion of regularization, the objective function is

$$\min_{\mathbf{m}\in\mathbb{R}^n} \ \phi(\mathbf{m}) = \phi_d(\mathbf{m}) + \beta\phi_m(\mathbf{m}) \tag{6}$$

where β is a weighting term beteewn the residual and regularization term. In cases where additional information or constraints are known, the objective function can be extended to include other terms

$$\min_{\mathbf{m}\in\mathbb{R}^n} \ \phi(\mathbf{m}) = \phi_d(\mathbf{m}) + \sum \beta_i\phi_{m_i}(\mathbf{m}) \tag{7}$$

where β is a trade off term between regularization functions. Examples of these regularization functions include smoothness and smallness. At the macro scale, the inversion problem is solved using a iterative least squares method with a Gauss-Newton solver [13]. Other non-iterative methods such as the Truncated Singular Value Decomposition [14], [15] have been used with the trade-off of spatial resolution and robustness [16].

Deep learning methods have emerged as transformative tools in various fields, including inversion of electrical resistive tomography data [10]. Deep learning methods aim to increase accuracy [17] and reduce computation time [10] compared to traditional inversion methods. One common approach in deep learning based inversion is to train an approximate generic inverse of the forward function. This inverse function $\tilde{F}^{-1}$, can then be used to estimate the model directly from data, that is

$$\mathbf{m} = \tilde{F}^{-1}(\mathbf{d}) \tag{8}$$

Another way deep learning can be integrated into inversion is by training a regularization function R [18]. An inversion method can either be modelled as an approximate inverse $(\tilde{F}^{-1})$ or as a regularization function (R), i.e.

$$\phi_{m_i}(\mathbf{m}) = R(\mathbf{m}) \tag{9}$$

D. Limitations

Typical applications of Electrical Resistivity Tomography (ERT) are in large-scale geophysical surveys, where the technique is used to investigate subsurface structures by measuring the distribution of electrical resistivity across an area. Common challenges in ERT applications include limitations in electrode lead length, the labour-intensive process of setting up and conducting surveys, and potential interference from external electrical sources [19], which can affect the accuracy of measurements. A significant advantage in geophysical ERT surveys is the ability to use multiple (2, 3 or 4) electrodes, and the flexibility to use a variety of electrode array configurations [20] e.g., gradient, dipole-dipole, Schlumberger,

Wenner arrays. These configurations reduce the effect of contact resistance and may improve the signal to noise ratio. In contrast, dual-probe Atomic Force Microscopy offers fewer measurement options. One key limitation is the uncertainty in contact resistance between the probe and sample surface, which is generally unknown. For the purpose of this study, the contact resistance is assumed to be small compared to the sample resistivity.

E. Dual Probe AFM Requirements

Getting information about the subsurface is reliant on the electrical measurements on the surface and topography of the surface, which can be determined using standard AFM imaging modes. A prototype survey grid is created, consisting of evenly spaced points set at a fixed height above the sample surface. Once established, this grid is draped over the actual topography of the sample. The application of ERT in AFM requires two electrodes that can be positioned independently. This approach contrasts with other electrical tomographic techniques in industrial [21] or medical [22] applications, where electrode locations are fixed and multiplexed. This requirement also excludes the use of single AFM probe arrays [23], as the distance between the electrodes would be fixed.

III. Existing Numerical Methods

This section describes existing ERT numerical methods and their evolution.

A. Forward Model Simulation

The forward model in Eq. 1 can be solved numerically using finite element solvers, such as COMSOL [24] or ANSYS [25]. However, specialized tools for large-scale ERT are also available, including SimPEG [26]. SimPEG was chosen for simulation due to its versatility in addressing ERT problems and the built-in 'Occam's Inversion' solver.

B. Occam's Inversion

Occam's inversion [27] is a generic algorithm for solving inverse problems, including ERT inversion. Occam's inversion iteratively minimises an objective function to solve an ERT problem. Other non-iterative solvers such as truncated singular value decomposition [16] have also been used however, these generally result in a lower spatial resolution.

IV. Hybrid Inversion Method

This section introduces an inversion method and compares efficacy to other methods.

A. Learnt Inversion

Learnt inversion methods cover the growing field of deep learning methods used to invert electrical tomography data including neural networks [28], convolutional neural networks [29] and UNets [30]. These methods provide greater contrast and stability when compared to Occam's inversion. A disadvantage of learnt inversion methods is the unpredictable results that may occur if the measured data is not within the training set. Furthermore, learnt inversion methods have fixed input and output vector sizes. If the model mesh, survey or underlining equations change, the inverse solver will need to be retrained.

B. Hybrid Learnt Inversion

The proposed inversion method is a hybrid approach that combines elements of traditional inversion methods with deep learning techniques to enhance accuracy and adaptability. The approach begins by applying the initial ERT measurements to an approximate inverse network, which is a neural network trained to estimate the resistivity distribution. This estimate is then evaluated against an objective function, which scores the quality of the inversion based on predefined criteria, such as the accuracy representing the resistivity distribution. Once the approximate inverse network provides an initial estimate, the model transitions into a traditional iterative inversion process. Here, the inversion is refined iteratively, incorporating adjustments based on discrepancies between the model and measured data. This iterative process continues until the inversion reaches a predetermined level of accuracy or a maximum number of iterations. The hybrid method seen in Figure 3 is particularly advantageous in handling complex subsurface features where resistivity patterns deviate from previously observed models. By leveraging the deep learning method's capacity to generalize from diverse data and traditional inversion's rigorous refinement, this approach is expected to be more adaptable to unpredictable or novel resistivity structures.

V. Simulation Results

A collection of subsurface scenarios were created to test the limits of the subsurface imaging techniques. A 1 μm^3 sample was prepared with a buried cube. The electrode locations were fixed at 8 nm intervals along the surface of the sample as shown in Figure 2. A series of parameters were altered including

1) Feature Depth
2) Feature Size
3) Resistivity Ratios
4) Measurement Noise

The simulation results can be evaluated qualitatively using recovered images, such as those in Figure 4 or quantitatively using the objective function. The recovered image may experience more artifacts, but provides information on the size, shape and location of objects. The objective function only provides insight on how reproducible the resistance measurements are from a particular model. The comparison between noise, depth and feature size to objective function can be found in Figures: 5, 6, 7 respectively. The objective function is improved by approximately 1.5 times if the background resistivity is smaller then the feature resistivity.

VI. Conclusion

In this study, electrical resistivity tomography is investigated for subsurface imaging using a dual-probe atomic force microscope. The proposed hybrid inversion method was observed to

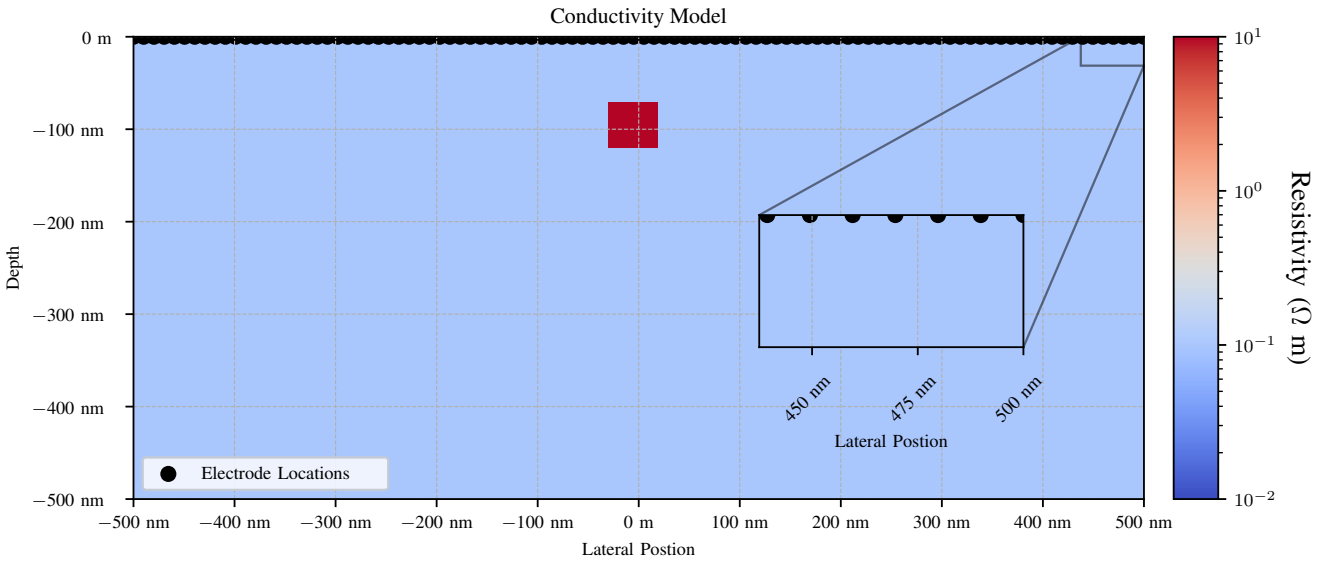

Fig. 2: 50nm sided cube buried within a high resistivity background with probe locations drawn on top. Contrast is resistivity

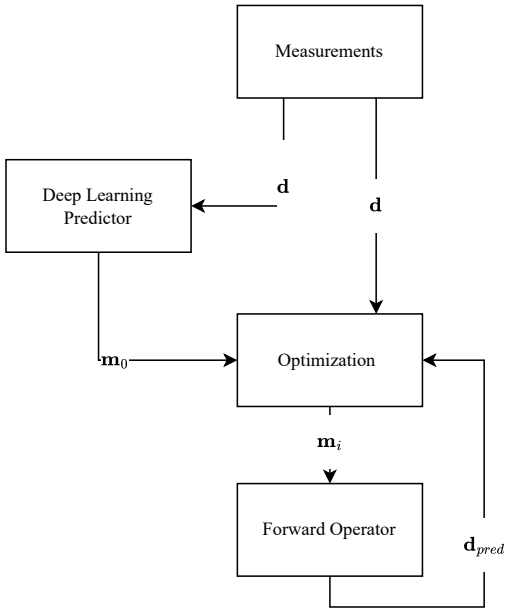

Fig. 3: Hybrid inversion block diagram with the input measurements $\mathbf{d}$ and recovered model $\mathbf{m}_i$. The initial estimate is from the deep learning predictor and further estimates are calculated recursively

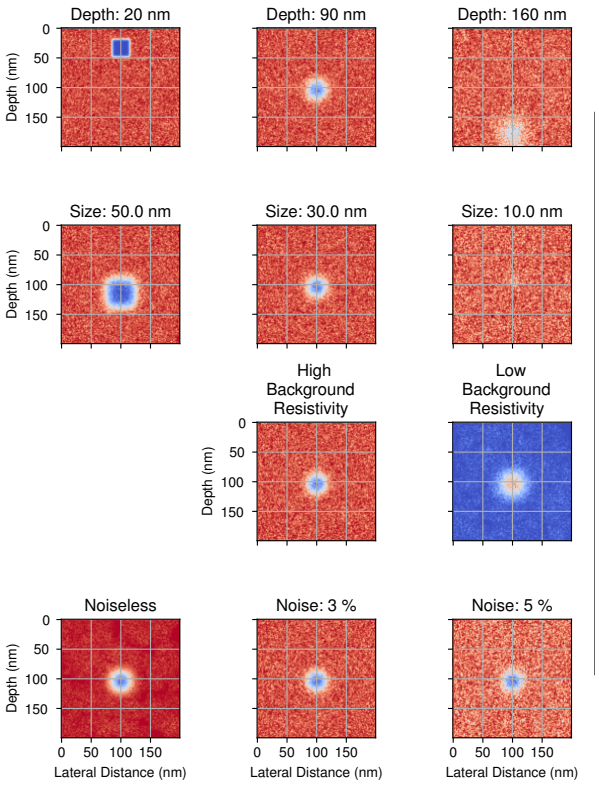

Fig. 4: Recovered resistivity models where the rows investigate the sensitivity of performance to depth, feature size, background resistivity, and measurement noise.

successfully image a 30nm cube to a depth of approximately 100nm in the presence of up to 5% measurement noise. These results show sufficient promise to warrant experimental validation. Future work will involve refining the reconstruction algorithm, dealing with contact resistance, and constructing the dual-probe AFM instrument.

VII. Acknowledgements

This project was supported by the Australian Research Council grant DP210103383.

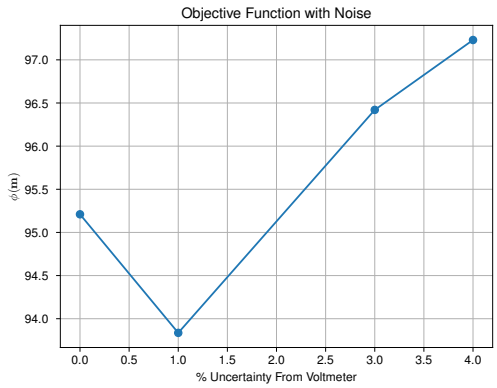

Fig. 5: Objective function versus voltmeter noise. Depth is fixed at 100 nm and size is fixed at 23 nm.

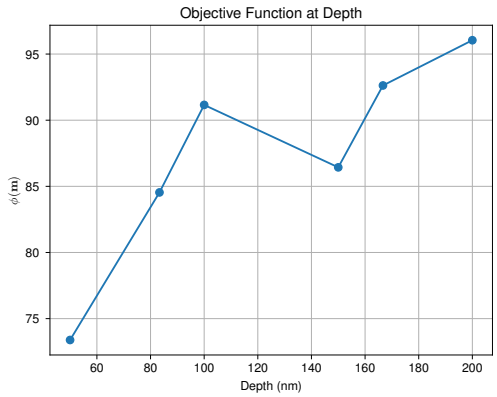

Fig. 6: Objective function versus depth. Size is fixed at 27 nm and there is no noise in the simulation.

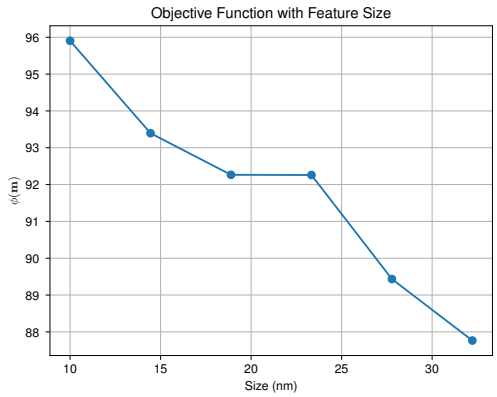

Fig. 7: Objective function versus feature size. Depth is fixed at 150 nm and there is no noise in the measurement.

References

[1] U. C. Wejinya, G. Shi, and A. Omolewu, "Afm based topography characterization of smooth, nanotextured, and microtextured surfaces," in *2018 IEEE 1st International Conference on Micro/Nano Sensors for AI, Healthcare, and Robotics (NSENS)*, 2018, pp. 60–63. DOI: 10.1109/NSENS.2018.8713637.

[2] J.-M. Breguet, W. Driesen, F. Kaegi, and T. Cimprich, "Applications of piezo-actuated micro-robots in microbiology and material science," in *2007 International Conference on Mechatronics and Automation*, 2007, pp. 57–62. DOI: 10.1109/ICMA.2007.4303516.

[3] M. Radmacher, "Measuring the elastic properties of biological samples with the afm," *IEEE Engineering in Medicine and Biology Magazine*, vol. 16, no. 2, pp. 47–57, 1997. DOI: 10.1109/51.582176.

[4] A. Imtiaz, T. M. Wallis, and P. Kabos, "Near-field scanning microwave microscopy: An emerging research tool for nanoscale metrology," *IEEE Microwave Magazine*, vol. 15, no. 1, pp. 52–64, 2014. DOI: 10.1109/MMM.2013.2288711.

[5] M. Soliman, Y. Ding, and L. Tetard, "Nanoscale subsurface imaging," *Journal of Physics: Condensed Matter*, vol. 29, no. 17, p. 173 001, 2017. DOI: 10.1088/1361-648X/aa5b4a.

[6] L. Collins *et al.*, "Dual harmonic kelvin probe force microscopy for surface potential measurements of ferroelectrics," in *Proceedings of ISAF-ECAPD-PFM 2012*, 2012, pp. 1–4. DOI: 10.1109/ISAF.2012.6297845.

[7] M. J. Cadena *et al.*, "Sub-surface imaging of carbon nanotube–polymer composites using dynamic afm methods," *Nanotechnology*, vol. 24, no. 13, p. 135 706, 2013. DOI: 10.1088/0957-4484/24/13/135706.

[8] G. S. Shekhawat and V. P. Dravid, "Nanoscale imaging of buried structures via scanning near-field ultrasound holography," *Science*, vol. 310, no. 5745, pp. 89–92, 2005. DOI: 10.1126/science.1117694.

[9] L. Tetard *et al.*, "Elastic phase response of silica nanoparticles buried in soft matter," *Applied Physics Letters*, vol. 93, no. 13, 2008. DOI: 10.1063/1.2987460.

[10] B. Liu *et al.*, "Deep learning inversion of electrical resistivity data," *IEEE Transactions on Geoscience and Remote Sensing*, vol. 58, no. 8, pp. 5715–5728, 2020. DOI: 10.1109/TGRS.2020.2969040.

[11] S. C. Constable, R. L. Parker, and C. G. Constable, "Occam's inversion: A practical algorithm for generating smooth models from electromagnetic sounding data," *Geophysics*, vol. 52, no. 3, pp. 289–300, 1987.

[12] M. Pessel and D. Gibert, "Multiscale electrical impedance tomography," *Journal of Geophysical Research: Solid Earth*, vol. 108, no. B1, 2003. DOI: https://doi.org/10.1029/2001JB000233.

[13] M. Vauhkonen, D. Vadász, P. A. Karjalainen, E. Somersalo, and J. P. Kaipio, "Tikhonov regularization and prior information in electrical impedance tomography,"

IEEE transactions on medical imaging, vol. 17, no. 2, pp. 285–293, 1998. DOI: 10.1109/42.700740.

[14] P. Xu, "Truncated svd methods for discrete linear ill-posed problems," *Geophysical Journal International*, vol. 135, no. 2, pp. 505–514, 1998. DOI: 10.1046/j.1365-246X.1998.00652.x.

[15] N. Avis and D. Barber, "Image reconstruction using non-adjacent drive configurations (electric impedance tomography)," *Physiological measurement*, vol. 15, no. 2A, A153, 1994. DOI: 10.1088/0967-3334/15/2a/020.

[16] C. Dimas, V. Alimisis, N. Uzunoglu, and P. P. Sotiriadis, "Advances in electrical impedance tomography inverse problem solution methods: From traditional regularization to deep learning," *IEEE Access*, vol. 12, pp. 47 797–47 829, 2024. DOI: 10.1109/ACCESS.2024.3382939.

[17] B. Wilson, A. Singh, and A. Sethi, "Appraisal of resistivity inversion models with convolutional variational encoder–decoder network," *IEEE Transactions on Geoscience and Remote Sensing*, vol. 60, pp. 1–10, 2022. DOI: 10.1109/TGRS.2022.3217580.

[18] A. Xu and L. J. Heagy, "A test-time learning approach to reparameterize the geophysical inverse problem with a convolutional neural network," *IEEE Transactions on Geoscience and Remote Sensing*, vol. 62, pp. 1–12, 2024. DOI: 10.1109/TGRS.2024.3424659.

[19] R. C. Benson, R. A. Glaccum, and M. R. Noel, *Geophysical techniques for sensing buried wastes and waste migration*. Environmental Monitoring Systems Laboratory, Office of Research and …, 1982.

[20] M. E. Everett, "Electrical resistivity method," in *Near-Surface Applied Geophysics*. Cambridge University Press, 2013, pp. 70–103.

[21] Y. Ji, "Design and implementation of hardware system for electrical capacitance tomography," in *2009 First International Workshop on Education Technology and Computer Science*, vol. 1, 2009, pp. 588–593. DOI: 10.1109/ETCS.2009.139.

[22] A. M. Wicaksono and Basari, "Design of electrical impedance tomography (eit) for medical imaging application," in *2019 IEEE International Conference on Smart Instrumentation, Measurement and Application (ICSIMA)*, 2019, pp. 1–4. DOI: 10.1109/ICSIMA47653.2019.9057297.

[23] R. Fasching, Y. Tao, and F. Prinz, "Cantilever tip probe arrays for simultaneous secm and afm analysis," *Sensors and Actuators B: Chemical*, vol. 108, no. 1, pp. 964–972, 2005, Proceedings of the Tenth International Meeting on Chemical Sensors, ISSN: 0925-4005. DOI: https://doi.org/10.1016/j.snb.2004.10.058.

[24] O. A. Sanuade, J. O. Amosun, T. S. Fagbemigun, A. R. Oyebamiji, and K. D. Oyeyemi, "Direct current electrical resistivity forward modeling using comsol multiphysics," *Modeling Earth Systems and Environment*, vol. 7, pp. 117–123, 2021. DOI: 10.1007/s40808-020-00898-4.

[25] Z. Wang and W. Zhang, "Simulation study of electrical capacitance tomography," in *2011 Second International Conference on Mechanic Automation and Control Engineering*, 2011, pp. 7682–7685. DOI: 10.1109/MACE.2011.5988829.

[26] R. Cockett, S. Kang, L. J. Heagy, A. Pidlisecky, and D. W. Oldenburg, "Simpeg: An open source framework for simulation and gradient based parameter estimation in geophysical applications," *Computers & Geosciences*, vol. 85, pp. 142–154, 2015, ISSN: 0098-3004. DOI: https://doi.org/10.1016/j.cageo.2015.09.015.

[27] S. C. Constable, R. L. Parker, and C. G. Constable, "Occam's inversion; a practical algorithm for generating smooth models from electromagnetic sounding data," *Geophysics*, vol. 52, no. 3, pp. 289–300, Mar. 1987, ISSN: 0016-8033. DOI: 10.1190/1.1442303.

[28] A. Adler and R. Guardo, "A neural network image reconstruction technique for electrical impedance tomography," *IEEE Transactions on Medical Imaging*, vol. 13, no. 4, pp. 594–600, 1994. DOI: 10.1109/42.363109.

[29] C. Tan, S. Lv, F. Dong, and M. Takei, "Image reconstruction based on convolutional neural network for electrical resistance tomography," *IEEE Sensors Journal*, vol. 19, no. 1, pp. 196–204, 2019. DOI: 10.1109/JSEN.2018.2876411.

[30] Ł. Maciura, D. Wójcik, W. Rosa, T. Rymarczyk, and M. Maj, "Unet model in image reconstruction for electrical impedance tomography.," *Przeglad Elektrotechniczny*, vol. 98, no. 4, 2022. DOI: 10.15199/48.2022.04.26.